Journal of Applied Fluid Mechanics, Vol. 7, No. 3, pp. 493-502, 2014.
Available online at www.jafmonline.net, ISSN 1735-3572, EISSN 1735-3645.
DOI: 10.36884/jafm.7.03.19566

Numerical Study of Sinusoidal Temperature in Magneto-Convection

H. Jamai[1†], S. O. Fakhreddine[1] and H. Sammouda[2]

[1] *Laboratoire d'Energétique et des Transferts Thermique et Massique (LETTM), Département de Physique, Faculté des Sciences de Tunis*
[2] *Ecole Supérieure des Sciences et de Technologie de Hammam Sousse - Université de Sousse*

†Corresponding Author Email *hanene_jamai@yahoo.fr*

(Received April 10, 2013; accepted November 9, 2013)

ABSTRACT

In this paper we would like to present a numerical study of the effect of magnetic fields on natural convection (magneto-convection) flow of electrically conducting fluid. The 2D square cavity which was studied is subjected to a sinusoidal temperature conditions. The left and the right walls were respectively heated and cooled with a sinusoidal temperature while the top wall was kept thermally insulated. The equations are solved numerically by employing finite element method (MEF) using the software COMSOL Multiphysics. We presented the results in wide range of Hartmann number and Rayleigh number in terms of isotherm contours, velocities fields streamlines, , and in an average and local Nusselt number which varies sinusoidally. Our results are shown to be in good conformity with the available benchmark solutions.

Keywords Numerical study (MEF), Sinusoidal temperature, Magneto- convection.

NOMENCLATURE

B0	external magnetic field
Cp	specific heat
E	electric field intensity
e	unit vector for an external magnetic field
F	Lorentz force
$\vec{g}$	acceleration due to gravity
$\vec{J}$	electric current density
k	thermal conductivity of fluid
l	distance between hot and cold walls
P	dimensionless pressure
T	temperature
ΔT	temperature variation
t	time
U	velocity of the fluid
u, v	component of the velocity

Dimensionless numbers

Ha	Hartman number $B_0 l\,(\sigma_e/(\rho\nu))^{1/2}$
Nu	Nusselt number, ql/[k]
Pr	Prandtl number, ν/α
Ra	Rayleigh number, gβ(Th-Tc)l3/αν',

Greek symbols

α	thermal diffusivity of fluid
β	volumetric coefficient of expansion
Θ	dimensionless temperatur
μ	viscosity of fluid
ν	kinematic viscosity
ρ	density of fluid
ρe	electrical charge density
σe	electrical conductivity
ψe	scalar potential for an electric field

1. INTRODUCTION

The effect of magnetic field in liquids metals (magneto-convection) are the subject of a great number of researches. The interest in these flows lies in their presence in many natural and applied phenomena. 1993 The effect of magnetic field in natural convection in an inclined rectangular cavity for heated and cooled on the adjacent walls, have been illustrated by Ece and Buyuk (2006). Indeed, it may be noted that H. Ozoe, E. Maruo (1987), H. Ozoe, K. Okada(1989), J.P. Garandetand al 1992, and M. Venkatachalappa, C.K. Subbaraya (1993), have made attempts to acquire a general and essential understanding of flows and heat transfer characteristics in an enclosure in the presence of magnetic field. Their studies found that the magnetic field decreases the heat transfer rate. Rudraiah et al (1995), Alchaar et al (1995) have shown a specific

interest to focus on a natural convection within a rectangular enclosure with a magnetic field where one vertical wall is heated and another one cooled while the bottom and top walls are insulated. Recently,S. Sivasankaran *et al* (2011) have studied numerically the effect of magnetic field in mixed convection, with varying sinusoidal temperature distributions on vertical walls. The authors proved that heat transfer rate is affected by the phase deviations. The same phenomenon has been studied by Dulal Pal (2010), but with an exponential temperature distribution in the presence of magnetic field and with internal heat and viscous dissipation. It has been found that the increasing of Prandtl number decreases the skin-friction coefficient, while the increasing of magnetic field increases the local Nusselt number. F.Z. Kadi *et al* (2011) have studied the coupled magnetohydrodynamic and thermal problems using 2D finite element-finite volume method taking into account the movement of the fluid. Their results show the presence of fast transients and the oscillatory behavior in both the velocity and the pressure.

The effect of the magnetic field was also studied in porous mediums. Grosan *et al* (2009) studied the effects of magnetic field and the internal heat generation on natural convection flow in rectangular cavity filled with porous medium. In most studies the isothermal or isoflux thermal boundary conditions were applied to the side walls of enclosures. Dulal Pal and Sewli Chatterjee (2011) combined numerically Soret and Dufour effects in micropolar fluid. They proved that velocity profiles are strongly influenced by the magnetic field. The increasing of Dufour number, increases temperature profile but the increasing of Soret number increases the concentration distribution.

Magnetohydro-dynamic (MHD) natural convection flow in a rectangular cavity has been investigated by S. Mahmud, R.A. Fraser (2004) and F.Z. Kadid as well as S. Drid and R. Abdessemed (2011). In the same context Xiaohui Zhang and Mo Yang (2011) numerically investigated the simulations of combination of thermal and MHD convection in rectangular cavity filled with electrically conductive fluids to different values of Prandtl numbers. The isotherms are not centro-symmetric at any point in time and the Nusselt number oscillates accordingly. The impact of thermal radiation on the unsteady laminar convective MHD flow is subjected to an external uniform magnetic M.Turkyilmazoglu, (2011). Their study proved that the increasing of magnetic field affected the temperature profiles, but decreases the radial and azimuthal skin friction values. In the same context, M. Sathiyamoorthy and Ali Chamkha (2010) presented the effect of the magnetic field in MHD. Laminar flow in two-dimensional MHD natural convection within a liquid gallium was investigated in the existence of inclined magnetic field for different thermal boundary conditions. It was found in general that the application of the magnetic field reduces the convective heat transfer rate in the cavity for any inclined angle.

In the same way, metallurgical industry, cooling engines in nuclear industry and crystalline growth for the industry of the semiconductors generate several questions for controlling the stability of these flows (A. Yu. Gelfgat and P. Z. Bar-Yoseph 2001; Xiaoming Zhou, Hulin Huang 2010 ; J.S. Walkera, D. Henry; H. Ben Hadid 2002) .

Our study relates the magneto-convection in rectangular cavity with metal fluid Pr=0.054 .The cavity is subjected to a sinusoidal temperature gradient. The main object is to determine the influence of Hartmann number on deformation cell, temperature distributions within the cavity and heat transfer rates at the heated wall and in the entire cavity in terms of local and average Nusselt numbers respectively..

2. MATHEMATICAL MOODEL

Magneto-convection flow in square cavity is permeated by a uniform magnetic field B with magnitude $\vec{B} = B_0 \vec{e}y$ and formed by the conservation equations for momentum energy and Lorentz force. The fluid can be mechanically incompressible, but its volume can change with temperature. This is the main of the approximation that was first studied by Oberbeck and later by Boussinesq, known as Oberbeck–Boussinesq approximation. The viscous, radiation and joule heating effects are neglected. The magnetic Reynolds number is assumed to be small so that the induced magnetic field is neglected. The vertical walls of the cavity are subjected to two sinusoidal temperatures respectively high and cold, while the vertical walls are adiabatic Fig.1.

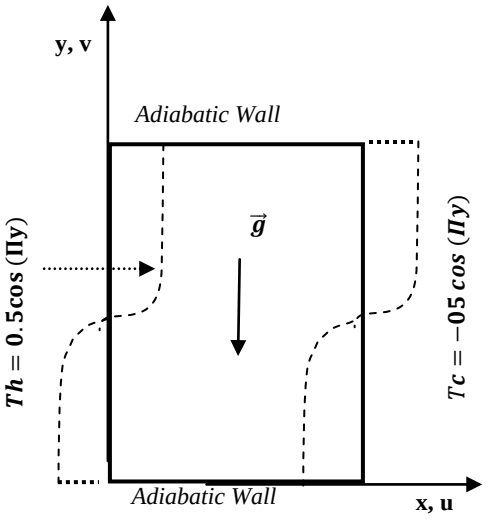

Fig. 1. Schematic diagram of the physical system

2.1 Equations

The Lorentz force term $\vec{F}$ is given as follows

$$\vec{F}' = \rho_e' \vec{E}' + \vec{j}' \times \vec{B}' \quad (1)$$

Where ρe is the electrical charge density of fluid, $\vec{E}$ the electric field intensity, $\vec{J}$ the electric current density and $\vec{B}$ the magnetic field.
Ohm's law holds for this system

$$\vec{J}' = \rho_e' \vec{U}' + \sigma_e (\vec{E}' + \vec{U}' \times \vec{B}') \quad (2)$$

Where σ_e and $\vec{U}$ are the electrical conductivity and the fluid velocity vector, respectively. The fluid is also assumed to be electrically neutral and the convective term $\rho_e \vec{U}$ is neglected in Ohm's equation. Then Eqs (1) and (2) become

$$\vec{F}' = \vec{J}' \times \vec{B}' \quad (3)$$

$$\vec{J}' = \sigma_e (\vec{E}' + \vec{U}' \times \vec{B}') \times \vec{B}' \quad (4)$$

Kobayashi (1986) introduced a scalar potential for an electric field:

$$\vec{E}' = -\vec{\nabla}' . \psi_e' \quad (5)$$

Then we have

$$\vec{J}' = \sigma_e (-\vec{\nabla}' \psi_e' + \vec{U}' \times \vec{B}') \quad (6)$$

The equation of continuity for electric current $\vec{J}$ gives.

$$\vec{\nabla}' . \vec{J}' = 0 \quad (7)$$

Equations (6) and (7) give:

$$\vec{\nabla}'^2 \psi_e' = \vec{\nabla}' . (\vec{U}' \times \vec{B}') \quad (8)$$

Under any specific external magnetic field $\vec{B}$, Eq.(8) gives the electric scalar potential. Both and the magnetic field B give a Lorentz force from Eq.(9)

$$\vec{F}' = -\sigma_e \vec{\nabla}' \psi_e' \times \vec{B}' + (\vec{U}' \times \vec{B}') \times \vec{B}' \quad (9)$$

The usual two-dimensional governing equations for the steady natural convection flow using conservation of mass, momentum and energy can be written as

$$\frac{\partial u'}{\partial x'} + \frac{\partial v'}{\partial z'} = 0 \quad (10)$$

$$\rho_0 \left(\frac{\partial u'}{\partial t'} + \left(u' \frac{\partial u'}{\partial x'} + v' \frac{\partial u'}{\partial y'} \right) \right) = -\frac{\partial P'}{\partial x'} + \mu \left(\frac{\partial^2 u'}{\partial x'^2} + \frac{\partial^2 u'}{\partial y'^2} \right) + (\vec{j}' \times \vec{B}') . \vec{i} \quad (11)$$

$$\rho_0 \left\{ \frac{\partial v'}{\partial t'} + \left(u' \frac{\partial v'}{\partial x'} + v' \frac{\partial v'}{\partial y'} \right) \right\} = -\frac{\partial P'}{\partial y'} + \mu \left(\frac{\partial^2 v'}{\partial x'^2} + \frac{\partial^2 v'}{\partial y'^2} \right) + (\vec{j}' \times \vec{B}') . \vec{j}' + \rho g \beta (T' - T_0) \quad (12)$$

$$\frac{\partial T}{\partial t'} + u' \frac{\partial T}{\partial x'} + v' \frac{\partial T}{\partial y'} = \alpha \left(\frac{\partial^2 T}{\partial x'^2} + \frac{\partial^2 T}{\partial y'^2} \right) \quad (13)$$

Using the following change of variable

$$(u, v) = \left(\frac{u'}{V_0}, \frac{v'}{V_0} \right) ; \; B = B_0 B'; \; P = \frac{P'}{P_0};$$

avec , $P_0 = l \sigma V_0 B_0^2$

$$\rho = \frac{l \sigma B_0^2}{V_0}; \; j = \sigma V_0 B_0; \varphi = l V_0 B_0;$$

$$\theta = \frac{(T - T_0)}{(T_h - T_c)} .; T_0 = \frac{(T_h + T_c)}{2},$$

$$x = \frac{x'}{l}; \quad y = \frac{y'}{l}; \quad t = \frac{t'}{t_0} \quad \text{avec}$$

$$t_0 = \frac{l}{V_0} \quad \text{et} \quad V_0 = \frac{\alpha}{l}$$

$$T = T0 \pm \frac{\Delta T \cos(\pi y)}{2},$$

$$Th = T0 + \frac{\Delta T \cos(\pi y)}{2},$$

$$Tc = T0 - \frac{\Delta T \cos(\pi y)}{2},$$

$$\theta = \frac{T - T0}{Th - Tc} = \pm \frac{\Delta T \cos(\pi y)}{2} \quad (14)$$

The governing equations reduce to non-dimensional form as:

$$\frac{\partial u}{\partial x} + \frac{\partial v}{\partial y} = 0 \quad (15)$$

$$\frac{\partial u}{\partial t} + \left(u \frac{\partial u}{\partial x} + v \frac{\partial u}{\partial y} \right) = -\frac{\partial P}{\partial x} + \Pr \left(\frac{\partial^2 u}{\partial x^2} + \frac{\partial^2 u}{\partial y^2} \right) - \Pr . Ha^2 v. \quad (16)$$

$$\frac{\partial v}{\partial t} + u \frac{\partial v}{\partial x} + v \frac{\partial v}{\partial y} = -\frac{\partial P}{\partial z} + \Pr \left(\frac{\partial^2 v}{\partial x^2} + \frac{\partial^2 v}{\partial y^2} \right) + \Pr . Ha^2 . u + (\Pr Ra) \theta \quad (17)$$

$$\Delta \varphi = \vec{\nabla} \left(\vec{U} \times \vec{e}_B \right) \quad (18)$$

$$\frac{\partial \theta}{\partial t} + u \frac{\partial \theta}{\partial x} + v \frac{\partial \theta}{\partial z} = \left(\frac{\partial^2 \theta}{\partial x^2} + \frac{\partial^2 \theta}{\partial y^2} \right) \quad (19)$$

The boundary conditions adopted for the resolution of the problem are:

Zero velocity on the walls. $u = v = 0$ (20)

Thermal Condition:

$$\begin{cases} \theta(0, y) = 0.5 \cos(y\pi) \\ \theta(1, y) = -0.5 \cos(y\pi), \\ \dfrac{\delta \theta}{\delta y}(x, 0) = \dfrac{\delta \theta}{\delta y}(x, 1) = 0 \end{cases} \quad (21)$$

Electrical conditions: electrical insulation

$$j.n = 0 \quad (22)$$

3 NUMERICAL METHOD AND VALIDATION

The governing equations along the boundary conditions are solved numerically using Comsol Multiphysics code which is based on the finite element method. This CODE is designed to simulate systems of coupled non-linear and time-dependent Partial Differential Equations PDE in one, two or three dimensions. Comsol Multiphysics can be used to simulate any system of coupled PDEs in the areas of heat transfer and fluid

dynamic. Some tests have been done in order to ensure that the results are independent both on the number of grid elements and on the value of the accuracy parameter. In more detail, Different mesh grids were tested by determining the amount of heat transferred (Average Nusselt number at the hot wall). Fig 2 shows that the results can be considered independent of the mesh from a number equal to 4896 mesh refined near the active walls. For each mesh variation, we tested the relative tolerance. We showed that the solution is converged when the error is less than 10-6. When the convergence criterion was applied here N_{dof} is the number of degrees of freedom, Ei is the estimated error in the current approximation to the component i. We point out here that Newton iteration is used for solving the non-linear equation system that arises in the steady-state case, whereas a method of lines discretization is used for the time-dependent case for the transient computations. At each time step, the convergence criterion was taken as where (U_i) is the solution vector corresponding to the solution at a certain time step. A_i is the absolute tolerance for the i the degree of freedom, and R is the relative tolerance for the computations, R = 0.01, Ai = 0.001 for i = 1,. . . , N_{dof} were used.

$$\sqrt{\frac{1}{N_{dof}}\sum_{i=1}^{N_{dof}}\left(\frac{|E_i|}{A_i+R|U_i|}\right)^2} < 1 \qquad (23)$$

After developing the model, the choice of parameters, and, in order to verify the accuracy of the numerical procedure, we have compared the obtained results for the case when magnetic field is absent (Ha= 0) in rectangular and for a Prandtl number Pr = 0.71. The Results obtained are shown in Fig.3 in comparison with those of Ranganathan Kumar and M. A. Kalam (1991) and those of M. Sankar, *et al* (1991) to the same conditions Fig.3. There is a good agreement between all these.

4. RESULTS AND DISCUSSION

In the present work, we inserted a metal liquid fluid with Prandtl number Pr=0.054 inside the sinusoidal temperature. The Rayleigh number (Ra) is varied from 10^3 to 10^6, Hartmann number (Ha) is varied from 0 to 100. The flow and temperature fields are presented in terms of streamline, isotherm contours and field velocity respectively. Later, heat transfer performance is examined in terms of average Nusselt number ($\overline{Nu}$) to predict the characteristics of magneto-convection.

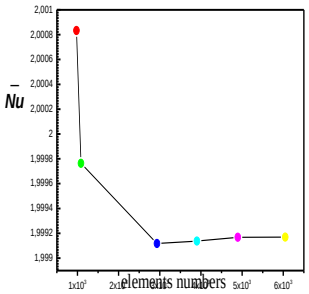

Fig. 2. Average Nusselt number for different element number and for Ha=20, Ra=10^4

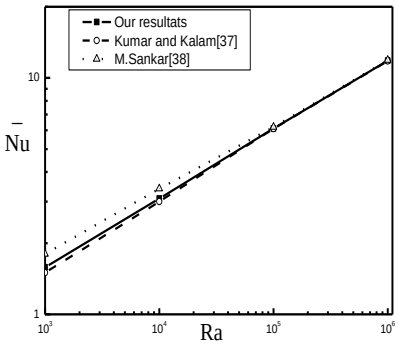

Fig. 3. Variation of average Nusselt number at the hfigot wall with Rayleigh number

4. 1 Effect of Rayleigh Number

The evolution of dynamic and thermal fields, whose configuration is such that the vertical walls are subjected to sinusoidal temperature condition for Ra = 10^3 to 10^6, are presented in Fig. 4 in the absence of magnetic field (Ha = 0). In different cases we noted the appearance of two counter-rotating cells at the top and bottom of the cavity. It should be noted that the two cells rotating in the top and bottom halves of the cavity are of the same importance in terms of intensity flow reflecting the anti-symmetry of the thermal boundary conditions. In both zones the fluid tends to rise along the hot wall and descends along the cold. However, in the middle of the horizontal cavity, the fluid charged by the two cells takes the same flow direction from left to right in such a way that the intensity is accentuated by the addition of shear forces which will lead to decrease on the thermal gradients in this region of the cavity. Indeed, the forces of volumes are proportional to the resulting thermal gradient imposed.

The effect of sinusoidal temperature on the dynamic structure of the flow is well illustrated by the profiles of vertical and horizontal velocities in the horizontal and vertical median planes respectively Fig.6 (a, b). This shows a peak near the vertical and horizontal walls, which is the consequence of high thermal gradients near the walls. In addition, the profiles of horizontal velocities show clearly the effect of shear stresses at the middle horizontal plane of the cavity and are reflected in rates much higher than those near the walls, especially for high Rayleigh numbers.
We notice also that the dynamic and thermal fields are symmetric in relation to the horizontal median plane of the enclosure. In addition, the isotherms show temperature gradients quite important especially at the middle horizontal plane of the cavity even for low values of Rayleigh number, i.e. where the forces are of less important volumes.

Indeed, this is explained by the fact that there are other forces in this region, which is of a dynamic nature and this is the shearing effect.

Similarly for low Rayleigh numbers (Ra <10^3), the flow is characterized by the presence of two cells stacked at the top and the bottom of the cavity with

a low flow rate which is confirmed by the values of the current function (Ra=10^3, ψ = 0.24). When we increase the Rayleigh number to Ra= 10^6 the flow intensity increases also. This is proved by the current function (ψ=18.21). Indeed, the increase of the volume of the forces leads to the development of dynamic boundary layers near the narrow cavity walls. Thermal boundary layers are well established and the thermal stratification dominates the entirety of the cavity, Fig.7(a, b) in relation to temperature profiles in horizontal and vertical mid-planes for different values of Ra.

4.2 Effect of Hartmann Number

Figure 5 shows the effect of magnetic field on the flow pattern and temperature distribution for Ra = 10^5 and for different values of Hartmann number Ha. In the absence of magnetic field Ha = 0, Fig.5(a), the flow exhibits two contra-rotatives circulating pattern rising along the hot wall and descending along the cold wall of the medium horizontal plane of the cavity.

It is interesting to note that as the structure of the flow ice qualitatively keeps the same structure of the presence of two counter-rotating recirculation, but the intensity of the flow decreases with the increase of Hartmann number Ha, which is well illustrated by Fig.5. Thus, the figure shows the attenuation of the intensity of the flow with increasing Hartmann number (Ha). However, the high shear in the middle of the cavity, encouraged by the fact that the two cells are counter-rotating, is mitigated by the presence of the magnetic field even for small values of Hartmann (Ha). Therefore, the presence of a magnetic field plays a stabilizing role In the absence of magnetic field Fig.5(a), the isotherms show a vertical stratification for the two cells, which indicates the strong thermal gradient. However, in the presence of a strong magnetic field when the Hartmann number increases, the intensity of the flow decreases as the magnetic force slows the flow up and down, which results in the horizontal stratification. This observation is well illustrated by Fig.8 (a, b) on the velocity profiles in median vertical and horizontal planes respectively.

4.3 Effect of Nusselt Number

Heat transfer results are presented in terms of Nusselt number Nu and average Nusselt number $\overline{Nu}$.

$$Nu = \frac{1}{\cos(\pi y)} \frac{\partial \theta}{\partial x} \tag{24}$$

$$\overline{Nu} = \int Nu \, dy \tag{25}$$

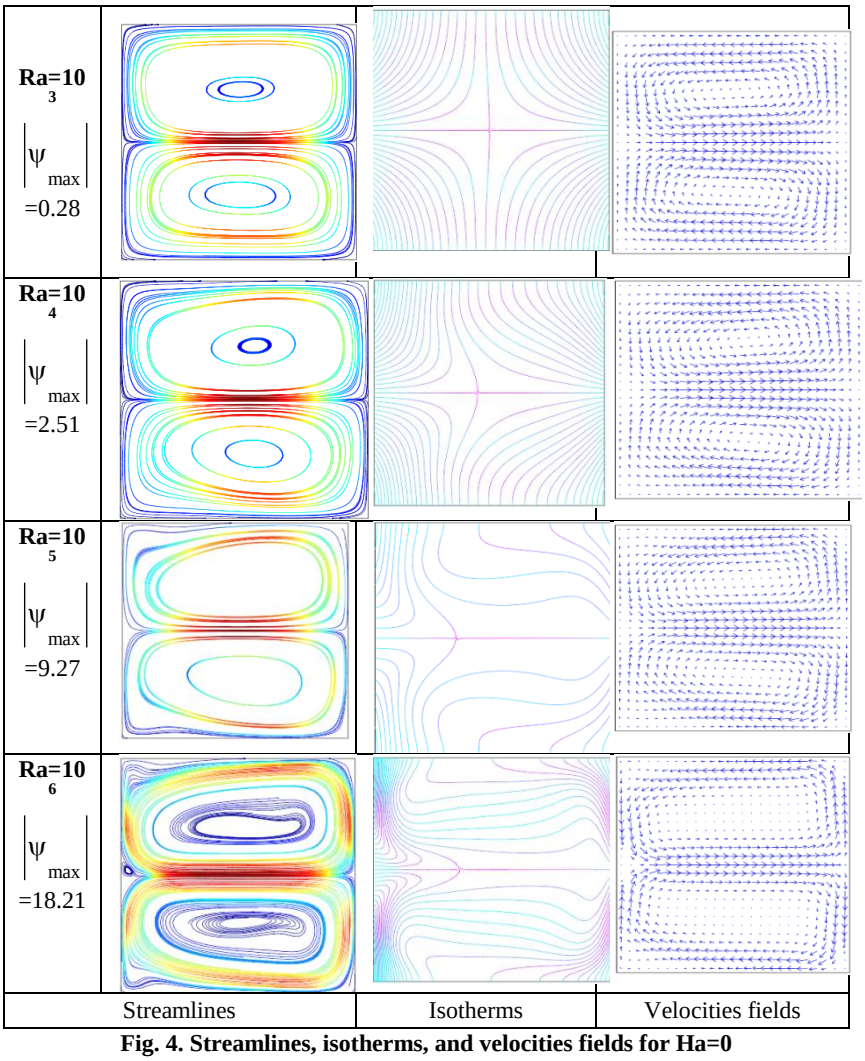

Fig. 4. Streamlines, isotherms, and velocities fields for Ha=0

In the absence of magnetic field, and varying the Rayleigh number, we find that the local Nusselt number (Nu) varies sinusoidally and presented two peaks near vertical walls. These peaks are increased by increasing the number of Rayleigh. In fact, the local Nusselt number takes its maximum value near the horizontal walls and decreases near the middle horizontal plane Fig.9 (a, b). But, in the presence of a magnetic field, qualitatively, the local Nusselt number remains the same structure, but the values are quantitatively less compared to those in the absence of magnetic Fig.9 (a, b).. The variation of average Nusselt number with Rayleigh number is shown walls in Fig. 11. It can be seen from the figure that the overall heat transfer rate increases as Ra increases, but, the average Nusselt decreases with increasing Hartmann number

We deduce that increasing the modulus of the magnetic field reduces heat transfer till it is inhibited. This is due to the fact that with the increase in Hartmann number the convection is progressively reduced by the magnetic drag, resulting in a lower heat transfer

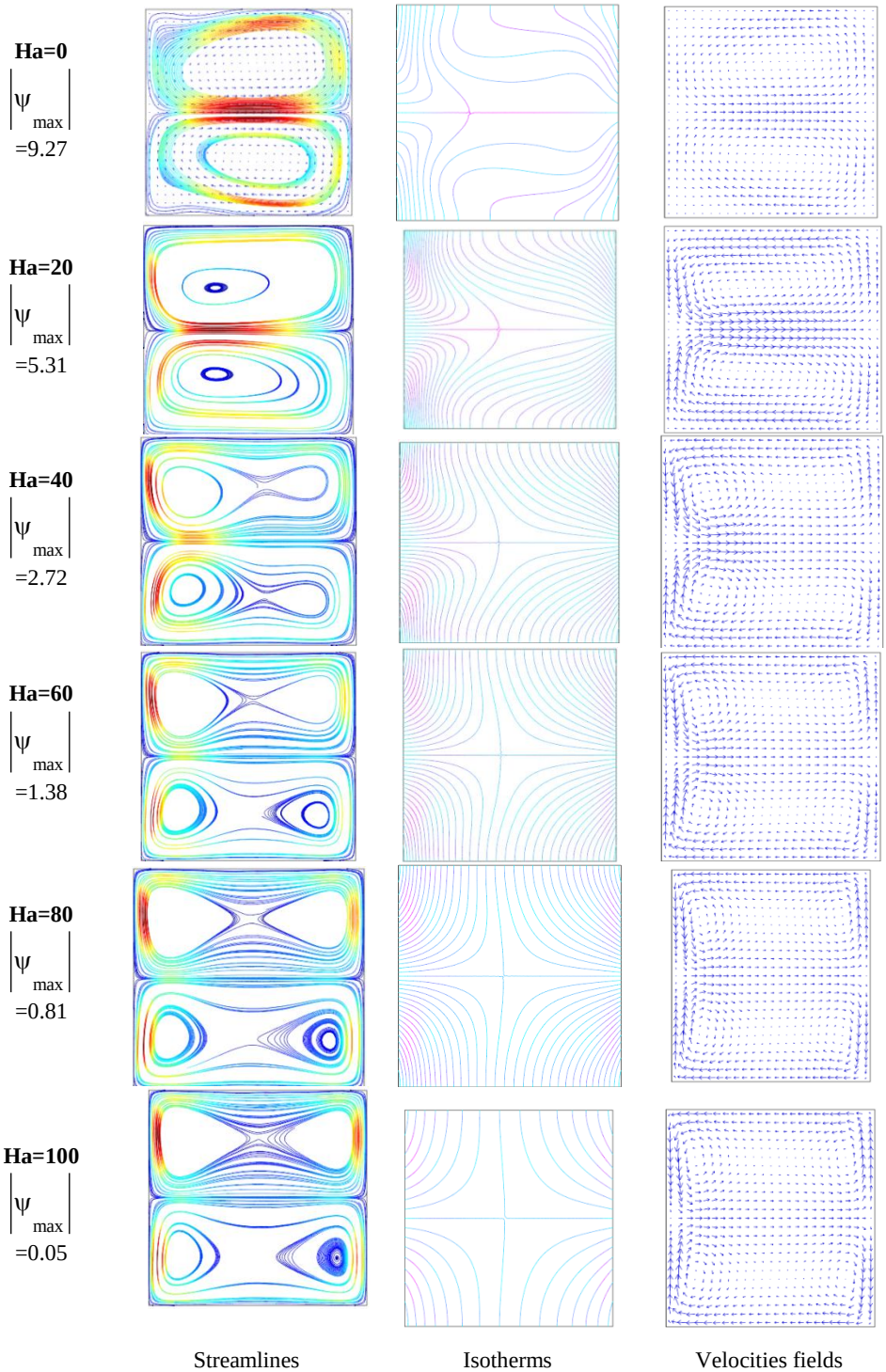

Fig. 5. streamlines, isotherms, velocities fields with Hartmann number variation for Ra=10^5

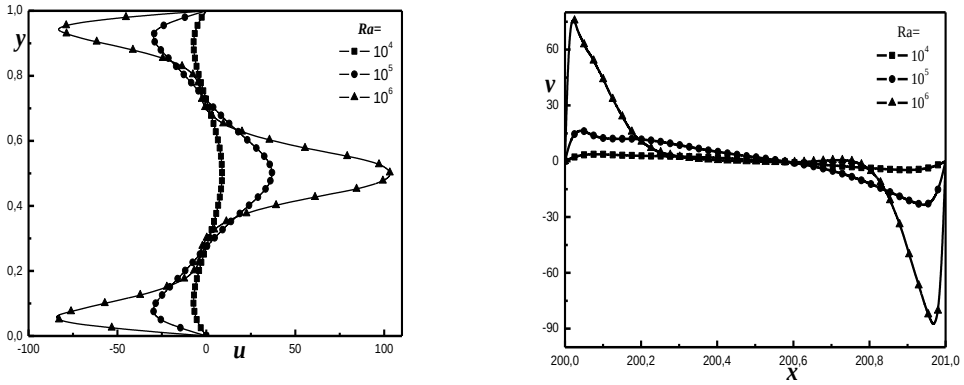

(a) **(b)**

Fig. 6. Horizontal velocity (a) and Vertical velocity (b) in median plane for Ha = 0

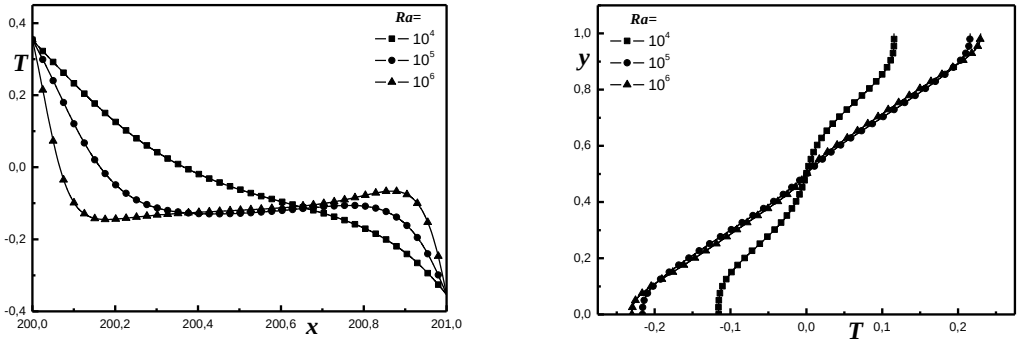

(a) **(b)**

Fig. 7. Horizontal (a)and Vertical (b)Temperature profiles for Ha=0

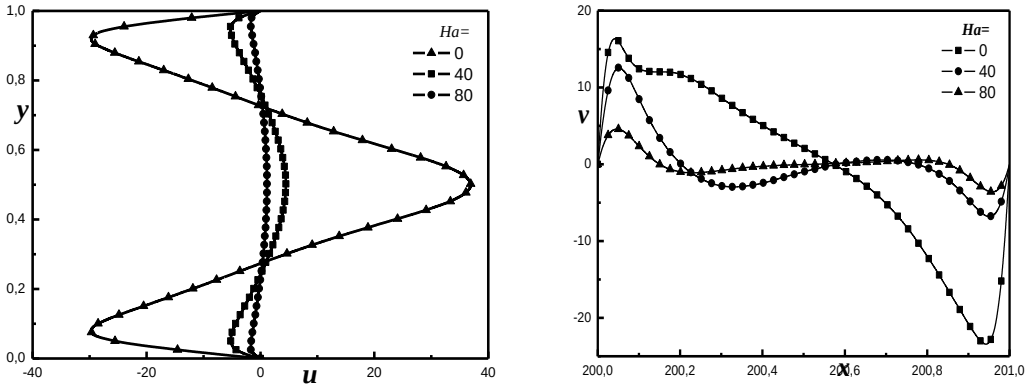

(a)

Fig. 8. Horizontal velocity (a) and Vertical velocity (b) in median plane for different values of Ha and Ra = 10^5

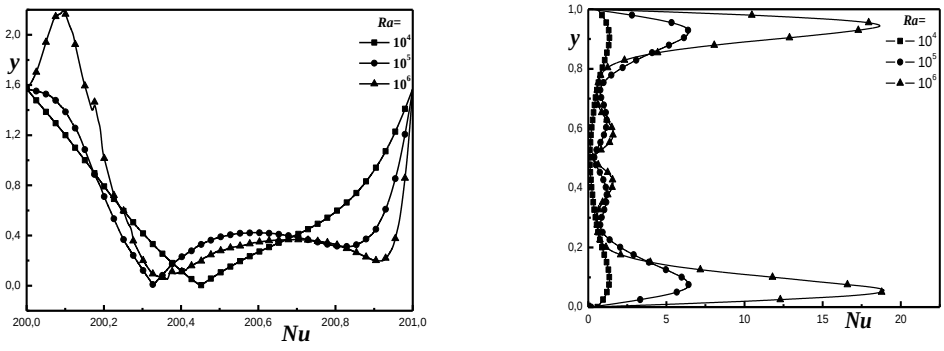

Fig. 9. Horizontal velocity (a) and Vertical velocity (b) in median plane for Ra =10^5

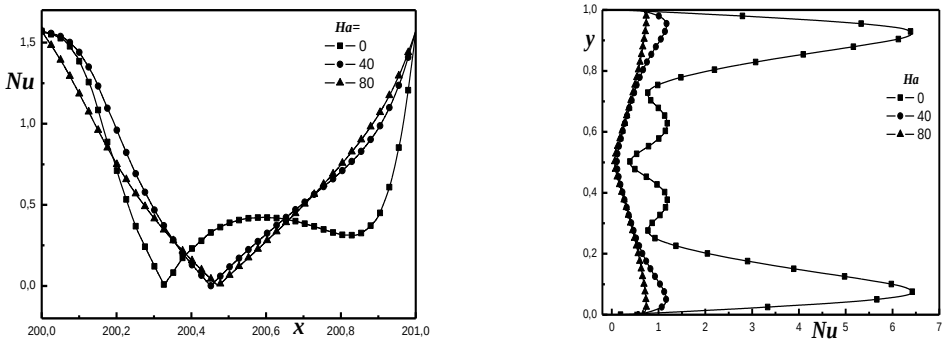

Fig. 10. Horizontal velocity (a) and Vertical velocity (b) in median plane for Ra = 10^5

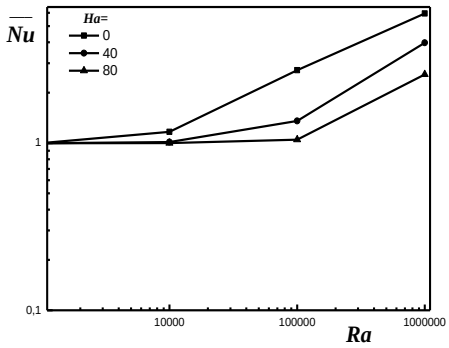

Fig. 11. Average Nusselt numbers for different Hartmann numbers

5. CONCLUSION

In this paper we have studied the coupled Magneto-convection and thermal problems using 2D Element-Finite method (MEF) made interesting by the effect of magnetic field in convection (Magneto-convection). The results show the effect of external magnetic field in both the velocity and Heat transfer. We conclude that the increasing of the Hartmann numb reduces Heat transfer.

REFERENCES

A. Yu. Gelfgat and P. Z. Bar-Yoseph (2001). The effect of an external magnetic field on oscillatory instability of convective flows in a rectangular cavity. *Phys. Fluids*, 13(8).

Comsol Multiphysics4.0 Laboratoire de Transfert Thermique et Massique(LETTM).

Dulal Pal (2010). Mixed convection heat transfer in the boundary layers on an exponentially stretching surface with magnetic field Applied Mathematics and

Dulal Pal, Sewli Chatterjee (2011).Mixed convection magnetohydrodynamic Heat and mass transfer past a stretching surface in a micropolar fluid-saturated porous medium under the influence of ohmic heating, Soret and Dufour effects. *Commun Nonlinear Sci Numer Simulat* 16 1329–1346.

F.Z. Kadid, S. Drid and R. Abdessemed (2011). Simulation of magnetohydrodynamic and thermal couplingin the Linear Induction MHD Pump. *Journal of Applied Fluid Mechanics*, 4(1). 1, 51-57, J.P.

J.S. Walkera, D. Henry, H. Ben Hadid (2002). Magnetic stabilization of the buoyant convection in the liquid-encapsulated Czochralski process.

H. Ozoe, E. Maruo (1987).Magnetic and gravitational natural convection of melted silicon e two-dimensional numerical computations for the rate of heat transfer. *JSME* 30, 774-784.

H. Ozoe, K. Okada (1989).The effect of the direction of the external magnetic field on the three-dimensional natural convection flow in a cubical enclosure. *International Journal of Heat and Mass Transfer* 32, 1939-1954.

M.C. Ece, E. Buyuk(2006). Natural convection flow under magnetic field in an inclined rectangular enclosure heated and cooled on adjacent walls. *Fluid Dynamics Research*, 38, 564-590.

Moreau (1992). Buoyancy driven convection in a rectangular enclosure with a transverse magnetic field. *International Journal of Heat and Mass Transfer* 35, 741-748.

M. Venkatachalappa, C.K. Subbaraya (1993). Natural convection in a rectangular enclosure in the presence of magnetic field with uniform heat flux from side walls. *Acta Mechanica*, 96, 13-26.

M. Turkyilmazoglu (2011). Thermal radiation effects on the time-Dependent MHD Permeable Flow Having Variable Viscosity. *International Journal of Thermal Sciences* 50, 88-96.

M. Sathiyamoorthy, Ali Chamkha (2010). Effect of magnetic field on natural convection flow in a liquid gallium filled square cavity for linearly heated side walls. *International Journal of Thermal Sciences*, 49 1856-1865.

M. Sankar , M. Venkatachalappa , I.S. Shivakumara (2006). Effect of magnetic field on natural convectionin a vertical cylindrical annulus.

T. J. Hurle, (1966). *International Journal of Engineering.*

N. Rudraiah, R.M. Barron, M. Venkatachalappa, C.K. Subbaraya (1995). Effect of magnetic field on free convection in a rectangular enclosure. *International Journal of Heat and Mass Transfer*, 33, 1075-1084.

Ranganathan Kumar and M. A. Kalam(1991) .Laminar thermal convection between vertical coaxial isothermal cylinders *International Journal of Heat and Mass Transfer*, 34(2), 513-524.

S.Alchaar, P. Vasseur, E. Bilgen (1995). Natural convection heat transfer in a rectangular enclosure with transverse magnetic field. *Journal of Heat Transfer e Transactions of the ASME* 117, 668-673.

S. Sivasankaran, A. Malleswaran , Jinho Lee , Pon Sundard2011. Hydro-magnetic combined convection in a lid-driven cavity with sinusoidal boundary conditions on both sidewalls . *International Journal of Heat and Mass Transfer* 54, 512–525.

S.C. Kakarantzas, I.E. Sarris, A.P. Grecos , N.S. Vlachos (2009). Magnetohydrodynamic natural convection in a vertical cylindrical cavity with sinusoidal upper wall temperature. *International Journal of Heat and Mass Transfer* 52, 250–259.

S. Kobayashi (1986). Effect of an external magnetic field on solute distribution in Czochralski grown crystals a theoretical analysis, *J. Crystal Growth* 75, 301-308.

S. Mahmud, R.A. Fraser (2004). Magneto - hydrodynamic free convection and entropy generation in a square cavity. International *Journal of Heat and Mass Transfer* 47, 3245-3256.

T. Grosan, C. Revnic, I. Pop, D.B. Ingham (2009). Magnetic field and internal heat generation effects on the free natural convection in a rectangular cavity filled with porous medium. *International Journal of Heat and Mass Transfer* 52, 1525-1533.

Xiaohui Zhang, Mo Yang (2011) .Unsteady numerical computation of combined thermally and electromagnetically driven convection in a rectangular cavity. *International Journal of Heat and Mass Transfer* 54, 717–721.